Microfluidic Platform for Culture and Live Cell Imaging of Cellular Microarrays

Team Members

Sarah Reichert (Team Leader)
Anthony Sprangers (Communicator)
Alex Johnson (BWIG)
John Byce (BSAC)

Client

Randolph Ashton, Ph.D.

Advisor

John Puccinelli, Ph.D.

December 14th, 2011

ABSTRACT

Neurodegenerative diseases, such as Parkinson's Disease, result from the loss of neuronal structure or function. Parkinson's disease affects 500,000 Americans and is caused by the loss of function in dopamine-releasing neurons [1]. Current therapies only lessen symptoms by replacing lost dopamine (DA), but do not treat underlying disease mechanisms [2]. Neural stem cells (NSCs) maintain the ability to differentiate into all types of neurons and stand to replace lost DA neurons and restore healthy DA levels in Parkinson's patients [3]. Differentiation of NSCs is primarily regulated by the features of the cellular microenvironment; one such characteristic is the localization and concentration of certain growth factors and other soluble molecules [4]. Dr. Randolph Ashton is seeking to eventually control differentiation of human pluripotent stem cells to treat these diseases. He has given us the challenge of finding a way to integrate cellular microarrays with microfluidic platforms so that the effects of various concentrations of soluble factors on neural differentiation can be tested in a high-throughput fashion. We designed and fabricated a microfluidic device that uses six Christmas tree microfluidic structures to generate concentration gradients of soluble molecules [6]. By adjusting this system to flow gradients over a cellular microarray, specific factors capable of instructing NSC differentiation can be tested in a high-throughput manner. This will allow for efficient identification of mechanisms related to neural differentiation and ultimately produce a homogenous population of neurons for regenerative medicine.

TABLE OF CONTENTS

INTRODUCTION

Client Description

Our client, Dr. Randolph Ashton, is an Assistant Professor in the Biomedical Engineering Department at the University of Wisconsin – Madison. His research focuses on regenerative stem cell medicines and how to transition these from the laboratory to clinical applications.

Background and Motivation

Neurons are responsible for processing and transmitting information between various parts of the body through electrical and chemical signaling. Typically, these mature nervous system cells have a limited proliferation capacity that continues to decrease with increasing age [1]. The limited amount of cell regeneration in the nervous system is devastating for patients suffering from neurodegenerative diseases, because their bodies are unable to replace neurons with compromised structures or functions. This is especially true with Parkinson's disease (PD), which results from the loss of function in midbrain dopaminergic neurons. Without neurons with the ability to properly release dopamine, these patients suffer decreased motor functions [2]. The National Institute of Health estimates that approximately 500,000 Americans currently suffer from PD, with another 50,000 new incidences occurring annually [3]. Presently, there is no cure for PD; current therapies only treat the symptoms, not the underlying dopaminergic neuron degeneration. Fortunately, promising research suggests that neural stem cells (NSCs) may eventually be used as a regenerative medicine for PD and other

neurodegenerative diseases, due to their ability to differentiate into all neuronal types [1]. Regenerative therapies using midbrain dopaminergic neurons differentiated from NSCs have been successful in mice as well as in initial human clinical studies [4]. Even though this approach seems promising for neurodegenerative diseases, many of the factors inducing neural differentiation are still unknown.

One of the factors that influences differentiation of NSCs *in vivo* is exposure to concentration gradients of soluble induction factors. Based on a cell's position within the gradient, gene expression and cell fate can be tightly controlled throughout neurogenesis. Therefore, a logical approach to evaluate which factors are important for neural differentiation is to test the effects of soluble factor gradients on NSCs. This knowledge could then be applied to help direct differentiation of NSCs in regenerative therapies. Through using standard cell culture techniques, assessing numerous concentrations of soluble factors would be extremely expensive and time consuming, as it would require large quantities of reagents and cells and extensive preparation times. An alternative approach to testing these gradients and analyzing their effects in a more high-throughput manner is the use of microfluidics.

Microfluidic devices utilize small channels containing minute amounts of solvents, samples, and reagents. Previous studies have shown their capability to generate accurate gradients of soluble factors using various techniques [5-10]. This makes microfluidic devices valuable for micro-scale high-throughput assays where several concentrations within a gradient can be evaluated for cell responses [11].

Typically, these devices are fabricated from poly(dimethylsiloxane) (PDMS) for several reasons, including its flexibility, cost effectiveness, ease of fabrication, accuracy, and optical transparency [11]. Microscale fluid dynamics is very different from fluid flow on the macroscale. Specifically, microfluidics allows for various phenomena such as laminar flow (Reynolds number less than 2300), which results in minimal diffusion between neighboring laminar streams containing differing soluble factor concentrations [12]. Laminar flow is well modeled through transport phenomena equations, making microfluidic strategies accurate and reproducible. Microfluidics also utilizes low flow rates, which can contribute to decreasing the amount of fluid shear stresses that cells within the devices are exposed to. This is important because shear stress has been shown to induce specific cell responses, such as cell morphology, which can ultimately alter cell fate [13].

Another beneficial aspect of microfluidics is their ease of incorporating cellular microarrays, which consist of hundreds to thousands of separate cellular colonies plated on a microscope coverslip [14]. The method for fabricating these microarrays can be seen in Figure 1; an example of a previously fabricated microarray is shown in Figure 2. This microarray approach is beneficial because many conditions can be tested simultaneously when incorporated into a gradient-generating microfluidic device. The cells in the microarray can be exposed to varying concentrations of soluble factors and changes in stem cell response (i.e. protein and gene expression) can be examined using immunofluorescence and polymerase chain reaction (PCR). The microarray approach allows for the isolation of a specific colony, which can then be expanded using standard cell culture

techniques [14]. It is also possible to integrate computer software into microfluidic systems to control inlet flow changes throughout experimentation. By automating microfluidics, cells within the microarray can be exposed to certain soluble factor concentrations for a set amount of time before being exposed to a different concentration. This approach better mimics an *in vivo* environment where cells experience a multitude of various soluble factors at varying time points.

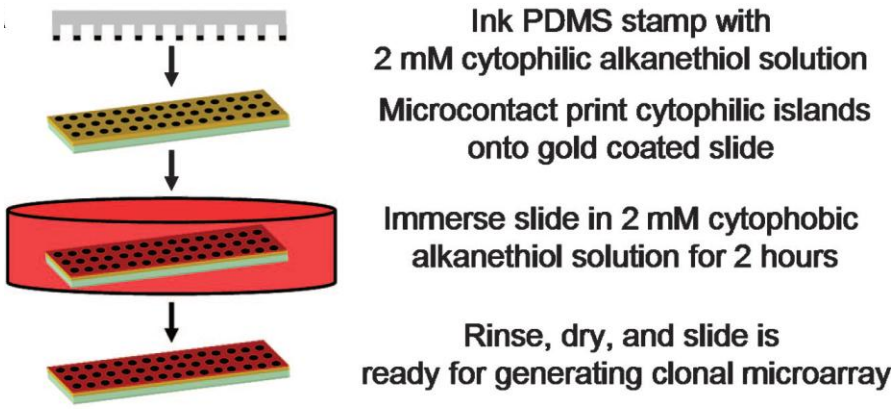

Figure 1: Fabrication of Cellular Microarrays. A PDMS stamp containing a cytophilic alkanethiol solution is microprinted on a gold coated slide, creating regions promoting cell adhesion. The gold slide is then immersed in a cytophobic solution, which inhibits cell adhesion. Thus, only the cytophillic regions will adhere cells while the cytophobic regions maintain cell colony isolation. Depending on the stamp area, hundreds to thousands of individual cell pixels can be created on a single microscope coverslip [14].

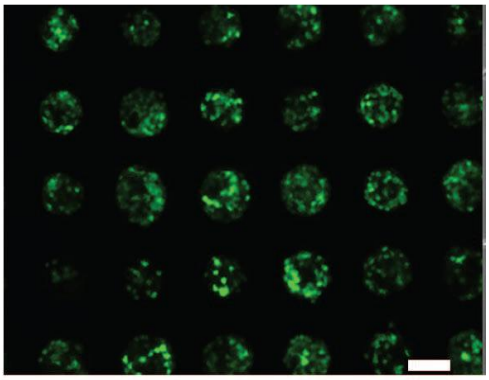

Figure 2: Cellular Microarray Pixels. Adult rat neural progenitor cell colonies expressing green fluorescent protein on a microarray. Scale bar = 100 μm [14].

The use of high-throughput methods, particularly cellular microarrays, in conjunction with a gradient-generating microfluidic device is an ideal platform for examining NSC differentiation. With this approach, it is possible to create accurate gradients and examine cell fate in a high-throughput fashion. This will allow for the determination of specific factor concentration ranges necessary to elicit certain NSC responses.

DESIGN REQUIREMENTS

The requirements for this project are outlined in the Product Design Specifications in Appendix A, and a few key constraints are highlighted here.

Integration with Microscope Stage

In order for the microfluidic platform to be imaged, it must fit precisely into the microscope stage. This requires that its dimensions are no greater than 158 mm in length and 105 mm in width. The piezoelectric positioning system of the microscope will also place a limitation on the weight on the device, with 0.5 kg being the absolute maximum.

Integration with Cellular Microarray

The cellular microarray will have a length of 24 mm and width of 60 mm, so the microfluidic platform must contain an opening that is 61 mm in width and 25 mm in length to enable the cellular microarray to be integrated. The extra 0.5 mm surrounding the array will help to ensure that it can be integrated and removed from the platform without damage to either device.

Microfluidic Constraints

To make the microfluidic platform as high-throughput as possible, it must be able to generate up to 60 discrete concentration conditions, each across 40 cellular colonies on the microarray. These specifications will allow for the determination of the soluble factor combinations and concentrations necessary to induce specific differentiation of NSCs. Lastly, the designed microfluidic platform must be capable of maintaining a reliable gradient throughout a typical experiment, which can last between one and ten days.

CURRENT DEVICES

The effects of soluble factor concentration gradients on cellular fates have been addressed through several research efforts. Within these efforts, multiple microfluidic devices have been developed to generate concentration gradients on a cellular scale for high-throughput analysis [10-13]. Each of the established methods is assessed in relation to the design constraints for this project in the Design Alternatives section of this paper.

Despite the wide use of gradient analysis, to our current knowledge no device exists that combines gradient generation with the specific design requirements of this project. The notable requirements that are novel in combination are the development of a flowing concentration gradient of multiple soluble factors across a removable microarray for long-term cell culture.

DESIGN ALTERNATIVES

Christmas Tree

The Christmas tree was first developed by Jeon *et al.* [13]. The device generates a gradient when two laminar fluid streams of differing concentrations enter the serpentine channels. The streams flow parallel to each other and mix by diffusion, creating one homogenous stream with a new intermediate concentration. The length of the serpentine channels must be designed to ensure adequate diffusive mixing of the two streams occurs. Mixing is dependent on flow rate, the diffusion coefficient, and residence time within the serpentine channel [5, 7].

The device is composed of a channel of networks consisting of horizontal channels, serpentine (or vertical) channels, and the broad channel, as shown in Figure 3A. Fluid with varying concentrations can be pumped through the separate inlets, as shown in Figure 3B [5, 7]. The resistivity of the horizontal channels can be neglected because the resistivity of the serpentine channels dominates due to their greater length and narrower width; this is advantageous when examining the flow of fluid through channels. All serpentine channels have the same dimensions, and thus the same resistance and fluid flux, which allows for well-defined flow throughout the entire network.

Using this design for gradient generation, the cellular microarray would be located within the broad channel. The width of the broad channel may have to be varied to accommodate for the cellular microarray, which may create problems with the structural support of PDMS. Dertinger *et al.* reported that the width of the broad

channel and sagging of the PDMS did not interfere with fluid flow [7]. However, Dertinger did not conduct long-term analysis of the device's function and reliability.

The use of this design would allow for the development of a well-defined gradient with simple control over fluid flow rate to vary the shear stress placed upon the cells. Generation of the gradient results in spatial resolution ranging from 2-20 μm between concentrations [5]. However, the width of the broad channel would limit the number of cellular pixels available for analysis.

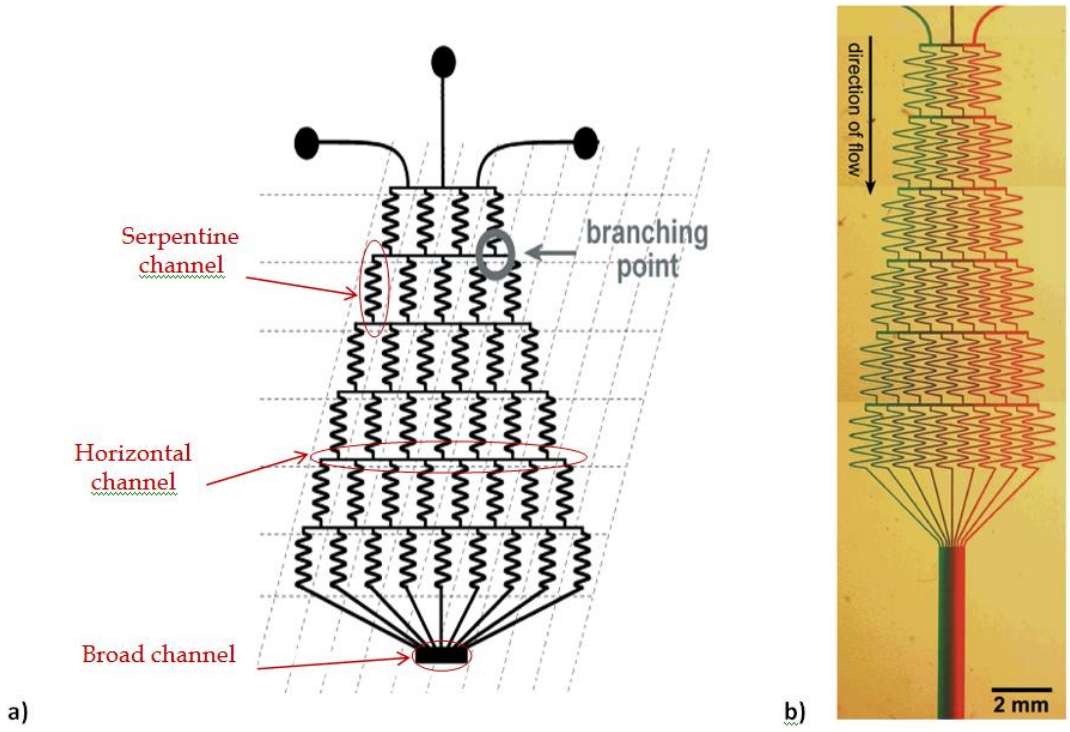

Figure 3: Christmas Tree Alternative. A: The Christmas tree design contains serpentine channels, horizontal channels, and broad channels. At a branching point, the fluid leaves the serpentine channel and splits within the horizontal channel. **B:** The gradient is established using red and green dyes. The gradient is maintained in the broad channel by laminar flow [5, 7].

Source/Sink Gradient Generator

The second design alternative for gradient generation is the Source/Sink Gradient Generator. To establish a concentration gradient, soluble factors injected

into the source region diffuse across the porous membrane into the channel by mass action diffusive transport [8]. Once in the channel, particles continue to diffuse toward the low concentration sink region, creating a concentration gradient within the channel. The concentration is highest nearest the source region and decreases with distance along the channel. To maintain the gradient and prevent equilibration, desired concentrations are maintained in both the source and sink regions by flowing fluid streams. This is also aided by the large relative volume of the sink region, which prevents accumulation of particles in the channel [8]. The channel where the gradient is constructed, however, does not experience any fluid flow. Because of the nature of gradient generation in this method, a transient period occurs when the gradient is being established. This may be problematic in a cell culture system where media in the channel must be changed. This approach may be beneficial for studying cell-cell communication, but it limits the transport of nutrients and waste to and from the cell, respectively.

This device is synthesized of PDMS using soft lithography and rapid prototyping. The Source/Sink Gradient Generator is assembled in three layers bonded together using plasma oxidation [8]. As shown in Figure 4, the top layer of the device contains a source, while the bottom layer contains a horizontal channel and relatively large sink region. The top and bottom layers are separated by a high resistance membrane constructed from polyester [8]. The high resistance of this membrane allows particle diffusion but resists fluid flow between the layers of PDMS. This device therefore establishes a concentration gradient without fluid flow between the input and output.

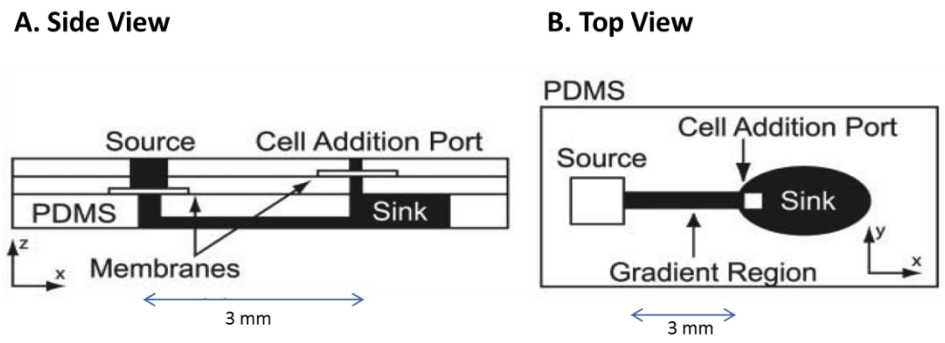

Figure 4: Source/Sink Gradient Generator. A: Side view of a multilayered source/sink orientation. The top layer (source) is separated from the bottom layer (sink) with a high resistance membrane. **B:** Top view layout of Source/Sink Gradient Generator. The gradient is generated in the channel connecting the source and the sink. This indicated cell addition port is designed so that cells can be added into the device after the gradient is established [8].

Universal Gradient Generator

The Universal Gradient Generator was designed using some of the same principles as the Christmas tree alternative. As seen in Figure 5, two or more input fluid streams enter the mixing channel where numerous flow dividers function to control the splitting and diffusive mixing of these streams in order to regulate the lateral transport of soluble factors and create a gradient. The output is an arbitrary monotonic gradient with various discrete concentrations that are dependent on the concentrations of the input solutions. Mathematical calculations can be performed to determine the proper placement of the flow dividers, and altering their locations can achieve a variety of user-defined gradient profiles [13].

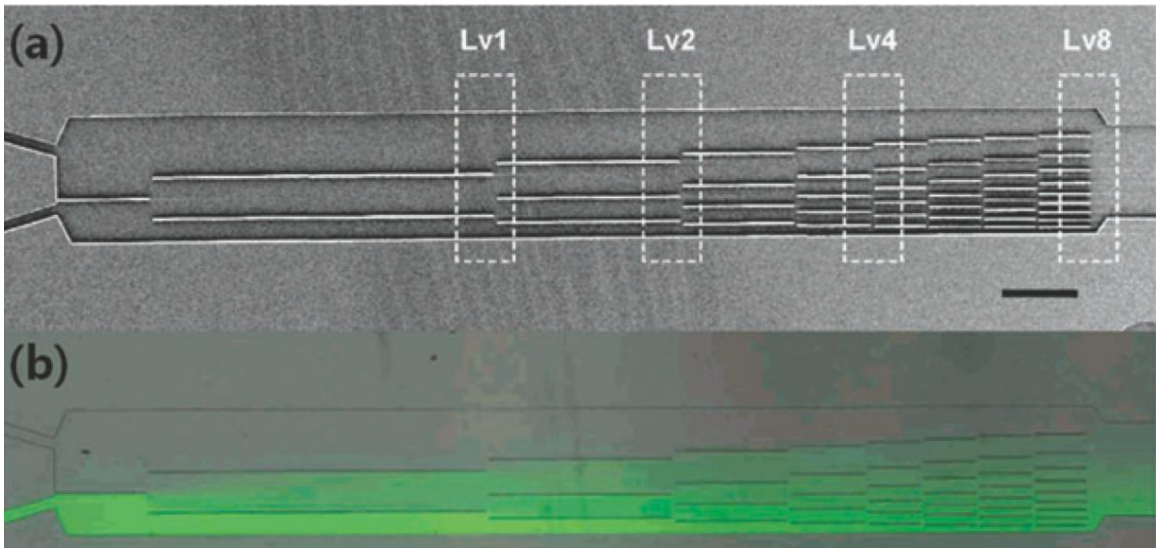

Figure 5: Universal Gradient Generator. A: This particular universal gradient generator has eight levels of flow dividers, which can be seen in this with scanning electron micrograph. **B:** Distribution of fluorescein isothiocyanate within the channel can be observed with fluorescence imaging. Scale bar is 500 μm [9].

One advantage of this design is that it does not have the same dead space that is associated with the serpentine channels of the Christmas tree alternative. Adding more inlets and rearranging the flow dividers can allow for extensive manipulation of the gradient profiles that are generated. However, like the Christmas tree, it requires significant volumes of input solutions in order to establish the concentration gradients and the cells within the microarray are still subjected to fluid flow [9]. A further challenge that this alternative would have in regards to our intended application is that scaling the output up to the size of the microarray would necessitate the mixing channel to be a significantly greater length. This could make both fabrication of the device and implementation with the microscope stage difficult.

Microjets Device

The final design alternative that was considered is the Microjets Device, shown in Figure 6. Microfluidic jets connect the source and sink compartments to the central cell culture reservoir and actively control the input of solutions into this area through pneumatic pressurization. The relative and absolute amounts of pressure that are applied through these microjets can be manipulated in order to alter the gradient profiles that are generated over the cultured cells. Within the cell culture area, no appreciable fluid flow occurs, so the gradient is established purely through diffusion [9]. Steady-state gradients can typically be formed with this alternative within 10 minutes. However, in order to maintain a reliable gradient, the source and sink outlets must be consistently supplied with fresh solutions so that the two constant concentration boundaries can be preserved. This design prevents the cultured cells from undergoing the forces associated with fluid flow and the open culture area enables gas exchange with the surrounding environment. Unfortunately, the microjets are prone to clogging, which can decrease the accuracy of the gradients that are established [9].

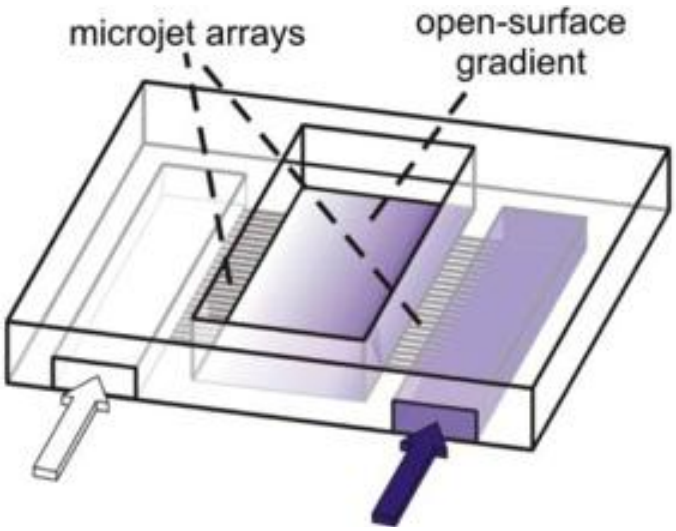

Figure 6: Microjets Device. Opposing arrays of microjects transport fluids from the source and sink chambers into the culture area, which is open to the surrounding environment. The microjects typically have cross-sections of 1.5 μm by 1.5 μm [8].

DESIGN MATRIX

We constructed a design matrix in order to compare the design alternatives and determine which approach was the most appropriate for use as a gradient generator in our final design. This analysis, included in Table 1, provided a quantitative means of assessing how well each alternative suited the needs of the project. The five criteria that were used to evaluate the alternatives were Ease of Fabrication, Accuracy of Gradients, Estimated Throughput, Ease of Use, and Ability to Integrate into the overall microfluidic platform. Based on the results of this matrix, we chose to pursue the Christmas tree alternative.

Table 1: Design Matrix. The weight of each evaluation category is indicated in the row headings, and the reasoning behind point allocations is described in the text. Based on the results of this design matrix, the Christmas tree alternative will be used as the gradient generator for the final design.

Category (Weight)	**Christmas Tree**	**Source/Sink Gradient Generator**	**Universal Gradient Generator**	**Microjets Device**
Ease of Fabrication (25)	22	20	20	20
Accuracy of Gradients (25)	21	17	18	18
Estimated Throughput (20)	20	15	16	15
Ease of Use (20)	20	20	15	17
Ability to Integrate (10)	8	3	6	5
Total (100)	**91**	**75**	**76**	**75**

Ease of Fabrication

Designing and fabricating microfluidic devices can be a relatively time-consuming process, which is why this category was allotted 25 of the total 100 points in the design matrix. Due to the high resolution required and numerous intricate steps that fabrication entails, the ideal final design would not significantly add to the complexity of this procedure. The Christmas tree alternative was designated 22 points in this category because it can be fabricated with only one layer of PDMS. The remaining alternatives only received 20 points each due to their requirement for complex fabrication and multiple layers, the latter of these being specific to the source/sink and microjets alternatives.

Accuracy of Gradients

The intended use of the device is to generate discrete concentrations of various soluble factors and allow them to interact with cultured cells to determine their effects on differentiation. As multiple factors may be used simultaneously, it is necessary that the gradients generated are accurate enough that the optimal levels of all the factors can be distinguished from other conditions. Accordingly, this category was weighted with 25 points. The Christmas tree received the most points because the lengths of the channels can be easily manipulated to ensure that adequate mixing occurs within them to generate an accurate final gradient. The other alternatives would have difficulties developing gradients that could span the desired width of the cellular microarray, which is why they received fewer points.

Estimated Throughput

One of the main goals of the project is to enable high-throughput analysis of cellular microarrays. It is desirable to be able to test multiple concentrations of growth factors simultaneously as well as maximize the number of cell pixels per condition. The Christmas tree alternative was the only option that received the full 20 points in this category. This is again due to the complications that would arise in attempting to scale the other alternatives up to the specifications for this project.

Ease of Use

The device should not be exceedingly difficult to operate, integrate with the microarray, separate from the microarray after use, or utilize with a standard microscope. Based on all of these considerations, the ease of use category was

designated 20 total points. The Microjets Device lost points in this category due to the challenges it poses with establishing the gradients. Similarly, the Universal Gradient Generator received less than the maximum amount of points due to the difficulty with incorporating it onto the microscope stage for imaging and analysis.

Ability to Integrate

In order for the device to be functional in establishing concentrations for eventual analysis, it must be able to be scaled to the specifications required for the project and reversibly integrated with the cellular microarray. Creating appropriately sized versions of all these alternatives to have flow over the entire microarray posed a problem, and the only option that had a readily available solution was the Christmas tree alternative. By dividing the broad channel into several discrete channels, the Christmas tree could be incorporated into the desired platform without a reduction in functionality. For this reason, it was awarded the most points in this category.

FINAL DESIGN

The final design prototype was centered upon a Christmas tree microfluidic gradient generator fabricated from PDMS. Synthesis of this device was conducted utilizing negative replica molding of a silicon master chip generated using soft photolithography. Unlike a conventional Christmas tree microfluidic device, the final design prototype did not contain output channels that converged into a single broad channel. Due to the aspect ratio of 2:1 (height:width) required for functional PDMS

synthesis, each output channel traverses the cellular microarray horizontally and houses a single row of cellular pixels on the array. This is depicted in Figure 7, in which a magnified image of the cell channel (350 µm wide) comfortably contains cellular pixels with diameters of 200 µm. These pixels will run along the entire cell channel for a total of 40 pixels per channel. Separate horizontal channels prevent diffusive mixing between adjacent concentration streams. Furthermore, with a simple modification to the design, the segregated channel structure allows researchers to analyze the contents of the cell media at each concentration.

Each cell channel is spaced 315 µm from adjacent channels to allow for accurate synthesis. Based on this spacing, a total of 60 rows of cell pixels are feasible on the cellular microarray. The final design will therefore contain 60 horizontal channels, each corresponding with one row of cell pixels on the microarray.

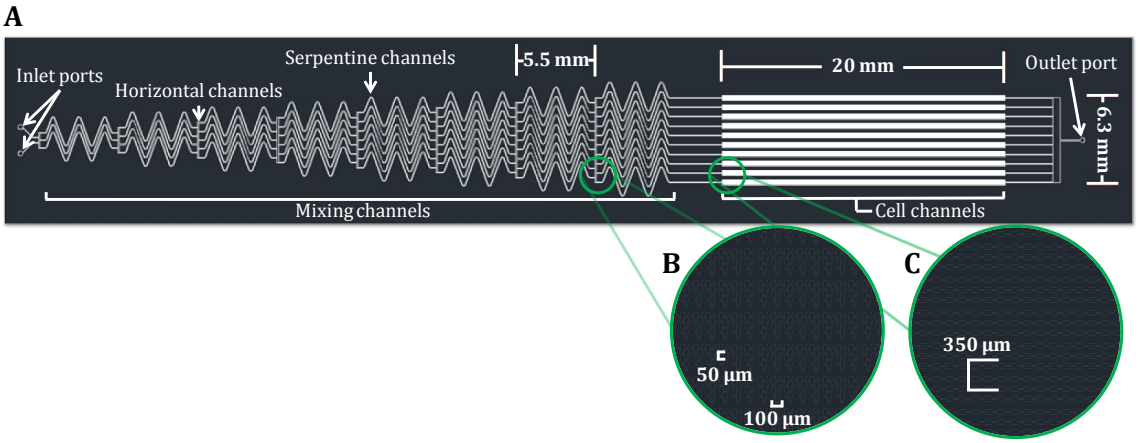

Figure 7: Christmas Tree Final Design. A: Magnification of one Christmas tree structure indicating the important features of the design. **B:** Further magnification of a horizontal channel that connects two serpentine channel levels. **C:** Further magnification of where the mixing channels convert to the singular concentration channels that will flow fluids over the cellular microarray.

A single Christmas tree with 60 channel outputs is not feasible due to the dimensional parameters of the microscope stage itself. The width required for such a large extent of branching is greater than that allotted in the design specifications. To correct this, the final design consists of six adjacent Christmas tree networks, as depicted in Figure 8A. This design allows for simultaneous analysis of multiple growth factors using a single microarray of cells. It would also allot for examination of varying time points of the presentation of soluble factors, giving the researcher the advantage of inspecting temporal separation. Lastly, the researcher is not limited to a single concentration range. Each independent Christmas tree network can be tailored to span a specific concentration range, enabling more refined analysis.

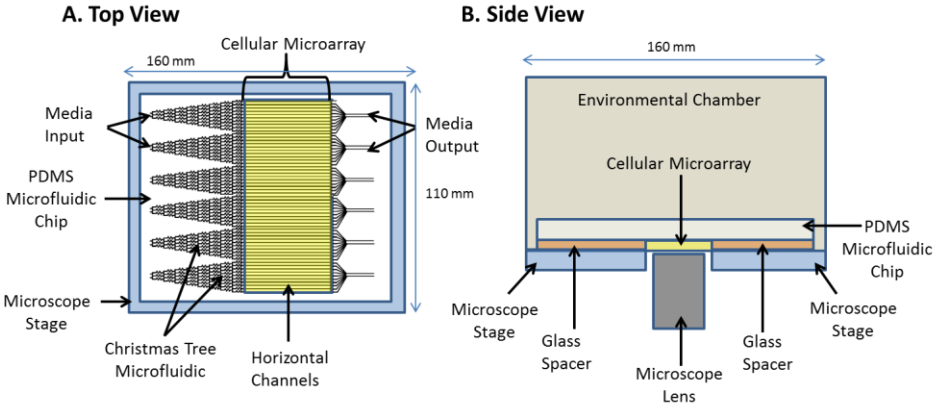

Figure 8: Integrating Design Components. A: Top view of the final design assembly. Output channels from the gradient generators flow horizontally across the cellular microarray (yellow). The entire design rests on a piezoelectric microscope stage. **B:** Side view of a potential integration scheme with the environmental chamber and microarray. The microarray is held between two glass spacers that are fused to PDMS with plasma oxidation.

Also shown in Figure 8A is the interface between the cellular microarray and the PDMS microfluidics device. To ensure each horizontal channel houses a single

row of cells on the cellular microarray, the array must be inserted with the same orientation during each experiment. The array must also be easily removed from the microfluidic chip for further analysis and culture after experimentation is complete. The details of this interface are part of the future work that is planned for this project, but a potential schematic showing glass spacers that perfectly flank and orient the cellular array is shown in Figure 8B.

The final design will also contain an environmental chamber to maintain physiological conditions during imaging and analysis. The integration of this component into the final design is also addressed as future work.

TESTING

Preliminary Integration

Our first testing objective was to determine if a PDMS mold could be successfully integrated with and removed from a glass coverslip without causing damage to either component. We obtained a prefabricated master from Dave Buschke of the Ogle lab and utilized negative replica molding to create a PDMS mold of this master. Then we pressed the mold onto glass coverslips that had the same specifications as the ones that will eventually be used to make the cellular microarrays. We found that the PDMS and glass coverslips could be physically adhered to and separated from one another without either device incurring damage, as shown in Figure 9.

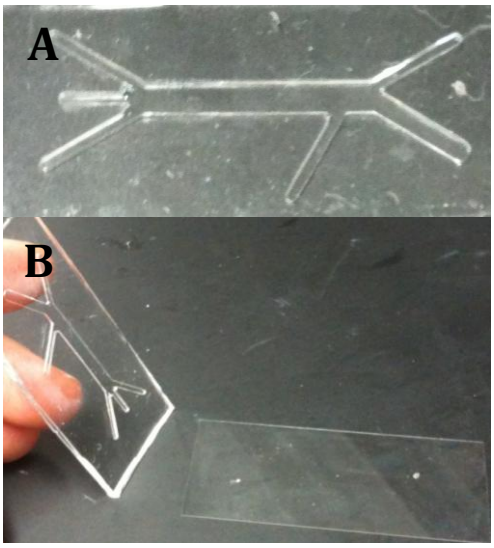

Figure 9: Integration and Separation of PDMS and glass coverslip. A: Pressing the PDMS onto a glass coverslip was accomplished without damage to either device. **B:** Separation of the PDMS and glass coverslip was done both by peeling away the PDMS and pulling on the glass, separately. Both methods demonstrated successful removal without breakage or other damage to either component.

The other portion of our preliminary integration testing was to establish whether the adhesive properties between unmodified PDMS and glass were enough to create a sufficient seal and prevent fluid from leaking from microfluidic channels. To do this, a PDMS device was pressed onto a glass coverslip with one inlet and outlet port exposed to allow air to escape from the channels when fluid was injected. A syringe was used to inject water, dyed with red food coloring, into the inlet. This allowed for qualitative confirmation that the inherent adhesion between PDMS and glass created an adequate seal for the prevention of fluid leakage, as shown in Figure 10.

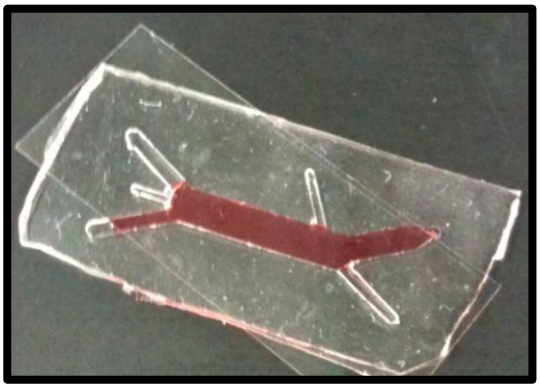

Figure 10: Injection of Dyed Water into PDMS. Exposing two ends of the channel to serve as an inlet and outlet allowed air to escape when water, dyed red with food coloring, was injected. No leaking was observed.

COMSOL Simulation

In order to assess the functionality of our proposed design prior to synthesis of a prototype, a computer simulation was conducted in COMSOL, a finite element analysis software program. COMSOL analysis was performed using a creeping flow model to observe the gradient produced between two inlets of different concentrations. As Reynolds number within the microscale system will be below 1, creep flow is expected within the channels. The simulation enacted using a mock soluble factor with a diffusivity of 1.0×10^{-11} m^2/s. The top input of a single Christmas tree was infused with 100 μM of the mock soluble factor in water, while the bottom input was infused with a simple water solution (0 μM). The respective solutions were then pushed through the channels simultaneously at 1.2 mm/s, although the velocity did not affect the simulation when the creeping flow condition was predetermined. The results of the analysis are included in Figure 11. This figure shows a magnified view of the ten horizontal cell culture channels of a single Christmas tree structure, with each color corresponding to a concentration value within that channel. As shown in the figure, the top channel displayed a

concentration of 100 μM, and the bottom channel contained a concentration of 0 μM. The remaining channels contained a linear concentration gradient that spans uniformly from the maximum value in the top to the minimum value in the bottom channel. This gradient adheres perfectly to the desired channel output. Based on the successful simulation, the final design prototype was constructed. Transport equations were performed to manually ensure proper diffusion would occur in the serpentine channels, as detailed in Appendix B. Transport equations were also utilized to ensure a low shear stress on incorporated cells, also in Appendix B.

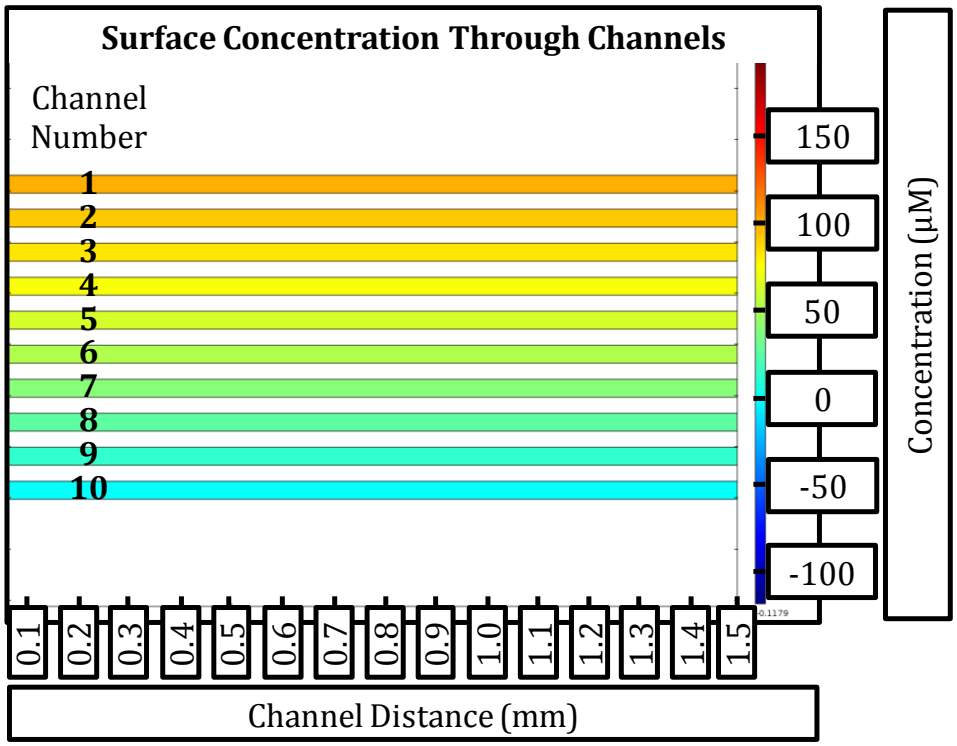

Figure 11: COMSOL Analysis to Verify Device Efficacy. Concentrations of 0 and 100 μM were input into the two inlets of one Christmas tree structure. Creeping flow was used to simulate the flow of fluids through the channels. The resulting concentrations in the cell channels are shown.

Experimental Device Testing

The first generation prototype was tested using both a qualitative analysis and quantitative assessment. The qualitative test was conducted primarily to

establish a test procedure for the quantitative analysis, as well as to assess device leakage and general functionality. The quantitative analysis that followed allowed for accurate assessment of the gradient generator and comparison to the theoretical simulation produced with COMSOL.

The qualitative test setup is shown below in Figure 12. To conduct this test, blue-dyed DIUF (deionized ultra-filtered) water was loaded into one 1 mL syringe, and red-dyed water into a second. A syringe pump then simultaneously pumped the solutions through tubing with a diameter of 1.016 mm and into each of two inputs of one Christmas tree structure of the microfluidic device at a flow rate of 3 μL/min. A single tube was inserted into the output of the Christmas tree, and the free end was fed into a collection beaker. Flow through the system was allowed until a visible gradient had been established. The gradient generated is visible in Figure 13. As shown in the figure, there is no visible leakage from the channels and the coloration of the generated gradient appears accurate.

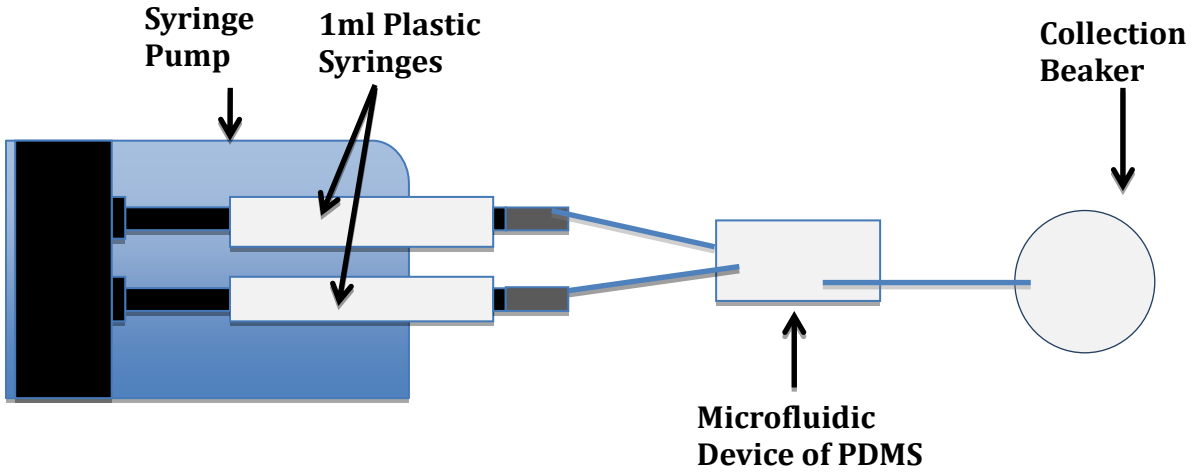

Figure 12: Experimental Setup up for Gradient Generation Testing. Top view of a schematic representation of the experimental setup used in qualitative and quantitative testing.

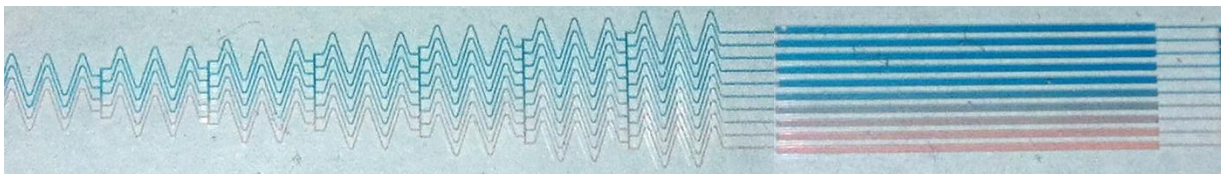

Figure 13: Qualitative Testing Results. Image of the concentration gradient generated after flowing two colored-water solutions through the experimental prototype.

Following qualitative testing, the same setup was repeated using fluorescence to enable imaging, analysis, and quantification of the gradient generated with the experimental device with a fluorescence microscope. One syringe in the fluorescent analysis was loaded with 100 μM fluorocein isothiocyanate (FITC)-labeled dextran (40 kDa), while the other contained a concentration of 0 μM. The solutions were again simultaneously pushed through a Christmas tree structure at a rate of 3 μL/min to generate a gradient in the cell culture channels. Following gradient generation, fluorescent images were taken of each channel. The fluorescent images are displayed below in Figure 14. Fluorescence intensity from three regions within each channel was measured and recorded as a percentage of the maximum channel fluorescence. The relative percentage of fluorescence corresponds to the relative percentage of concentration with respect to the maximum channel concentration.

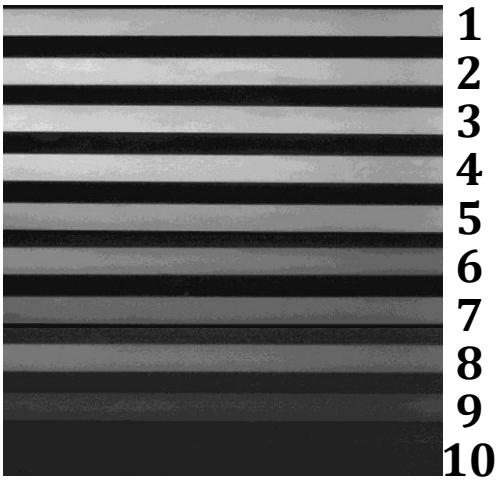

Figure 14: Qualitative Fluorescence Testing Results. Fluorescence testing with ultra-filtered deionized water (0 μM) and 100 μM dextran tagged with fluorescein isothiocyanate (FITC) input into the inlet ports at a rate of 3 μL/min. A fluorescence microscope was used to image the cell channels, shown in grayscale above.

Comparison of COMSOL Analysis and Experimental Device Testing

The relative fluorescence data was plotted along with relative concentration percentages produced in the theoretical COMSOL simulation, as shown in Figure 15. The quantitative fluorescent analysis adheres closely to the theoretical simulation, with the exception of the fluorescent signal observed in channels three and four. The increased fluorescence is likely due to a synthesis error in the PDMS microfluidic network, rather than saturation of the imaging device or to high of a flow rate. An error in the PDMS synthesis could cause a change in resistance in one of the channels, driving excessive flow into channels three and four. Although saturation at high concentrations of FITC-dextran could explain the increased signals in channels three and four, reduction of the maximum concentration at the input to 25 μM produced a similar result (data not shown). Similarly, an excessive flow rate could produce an improper gradient. This was also ruled out, as testing at

lower flow rates yielded a curve with similarly increased concentrations in channels three and four (data not shown).

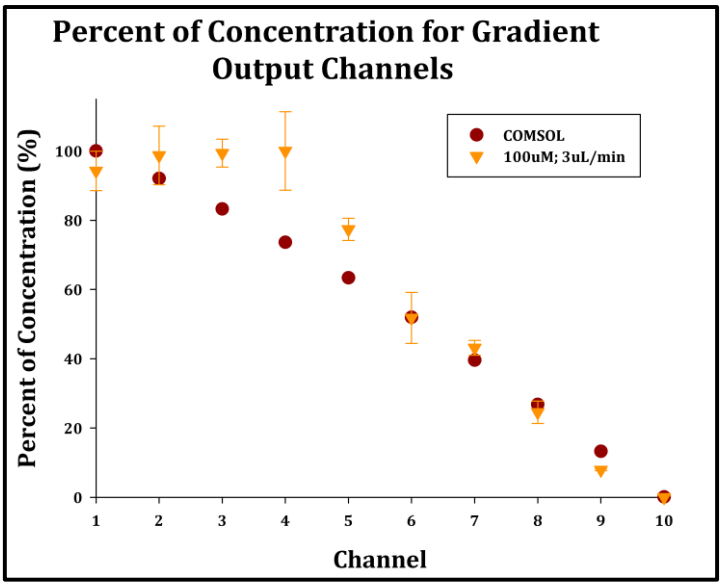

Figure 15: Comparison of COMSOL Analysis and Experimental Device Performance. A solution of 100 µM dextran-FITC was input into one inlet of the experimental device and ultra-filtered deionized water (0 µM) was input into the other, both at a rate of 3 µL/min. Fluorescence was measured at three locations in each of the cell channels, and averages were compared to the expected results based on COMSOL analysis. Parameters for the COMSOL analysis were corresponding 100 µM and 0 µM inlet concentrations and creep flow.

ETHICAL CONCERNS

As our device will be used for testing cell culture systems *in vitro,* the primary ethical concern is the collection and presentation of accurate data. Caution has been and will continue to be taken to ensure that experiments are conducted precisely and accurately to maintain the integrity of the produced results.

TIME MANAGEMENT

To create and test a functional prototype by the end of the semester, time management was an integral part of our design process. Our initial week-by-week

schedule and actual accomplishments throughout the semester are indicated in the Gannt chart shown in Table 2. The portion of the project that consumed the most time was the simulation and analysis of the proposed design in COMSOL. Although this initially delayed fabrication and testing, we were able to make up for the lost time and confirm device functionality and accuracy before the conclusion of the semester.

Table 2: Gannt Chart of Design Process. Although the actual accomplishments were not always achieved in the same order or in the same amount of time as originally planned, we managed to successfully fabricate and test an experimental device before the semester was over.

Tasks	September					October				November				December	
	2	9	16	23	30	7	14	21	28	4	11	18	25	2	9
Meetings															
Advisor	X	X	X	X	X	X	X	X	X	X		X	X	X	
Client	X	X	X	X		X		X	X	X	X	X			
Team			X	X	X		X							X	
Product Development															
Research	X	X	X	X	X	X	X		X	X	X	X	X	X	
Brainstorming		X	X	X	X	X			X	X	X				
Design Matrix						X									
Design Prototype						X	X	X	X	X	X	X	X		
Fabricate Prototype													X	X	
Testing										X			X	X	
Deliverables															
Progress Reports	X	X	X	X	X	X	X	X	X	X	X	X	X	X	X
PDS		X			X			X							X
Mid Semester PPT						X		X							
Mid Semester Report								X							
Final Report															X
Final Poster														X	
Website Updates	X	X	X	X	X	X	X	X	X	X	X	X	X	X	X

Colored boxes: projected timeline
X: accomplishments for the given week

COST ANALYSIS

Through our collaborations with the Ogle, Beebe, Williams, and Kreeger laboratories as well as the Chemistry Glass Shop at the University of Wisconsin-Madison, we were fortunate enough to have most of the materials used in this project donated. This was especially fortunate because we only utilized a small amount of materials to fabricate the masters and PDMS molds, but the minimum purchasing quantities for these items far exceeded these amounts. Having to purchase the excess materials would have significantly driven up the costs of the project. As shown in Table 3, the highest cost in our actual expenditures was the purchase and shipment of the photomask. In order to obtain the high resolution desired for the microfluidic device, we had the photomask made by Fineline Graphics in Denver, Colorado. This company is able to achieve resolutions at are an order of magnitude greater than local companies, with the tradeoff being the increase in price.

Table 3: Details of costs incurred through the course of the project. For the total cost, the actual amount paid is indicated in bold, with the projected cost if we would have had to purchase materials for master and mold fabrication indicated in parentheses.

Item	Cost
160 mm x 110 mm x 1 mm glass piece	$2.25*
Photomask + shipping	$245.02
SU-8 2025	$585.60’
Sylgard 184 Silicone Elastomer Kit	$73.79’
FITC-Dextran 40kDa	$78
Poster	$43.75
Total	**$366.77** ($1028.41)

*: Generously donated by the UW-Madison Chemistry Glass Shop
‘: Small samples generously donated by the Williams NITRO Lab

FUTURE WORK

Further development of this device will initially entail determining the cause of the unexpected results in fluorescence testing. Although error in synthesis is expected to be the primary problem for the results obtained, examination of the channels with a microscope will be used to determine if any blockages are present, due to particles or air bubbles, which could be the cause of uneven flow. To ensure no air is present within the device, the device can be purged with water or ethanol prior to experimental use. These techniques are expected to effectively clear the system and prevent the formation of air bubbles. To further minimize bubble formation, modifications will be made to the final design, as shown in Figure 16. This will entail changing the interface between the end of the serpentine channels and the start of the cell culture channels. Currently this interface involves a drastic channel width alteration from 50 to 350 microns, as shown in Figure 16A. We plan to taper this width change, Figure 16B, which will minimize bubble entrapment at the interface. Along with this modification, we will increase the length of the inlet and outlet ports which will allow for easier inlet and outlet tube incorporation. We also plan to change to a two-layer PDMS approach to increase channel height in the cell culture channels to 250 microns. This will effectively decrease fluid shear stress even more as fluid shear stress is inversely proportional to the height cubed.

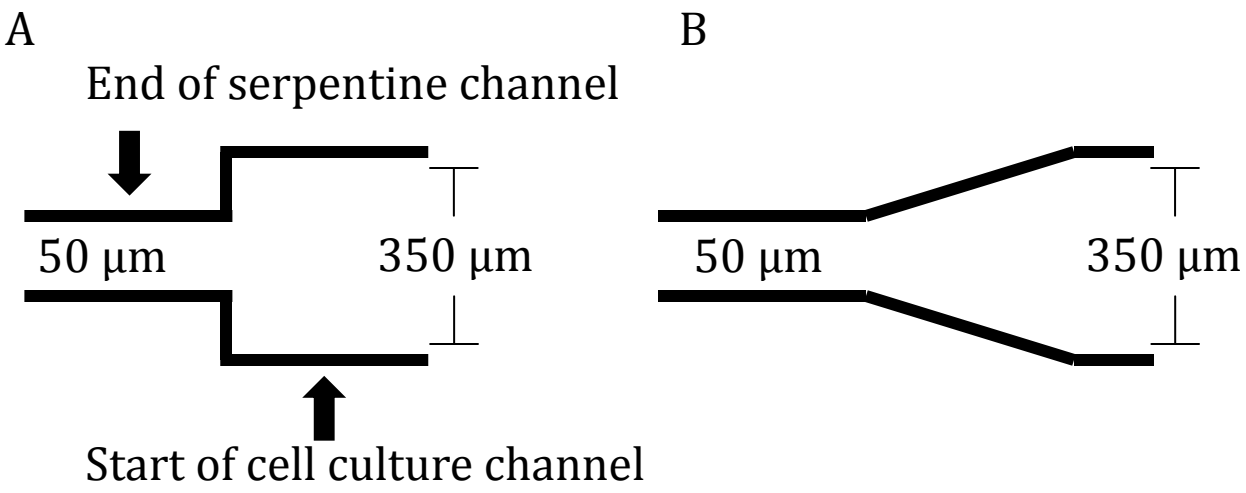

Figure 16: Future Modifications for Design. A: Current interface at the end of the serpentine channels and the beginning of the cell culture channels. This drastic size change has been the source of bubble problems within the microfluidic device. Future modifications will taper this change to **B**, which allows for a steadier size change.

Following these changes in our design, we will reevaluate fluorescence testing to ensure our device models the COMSOL analysis. After this we will examine the integration of the microarray with the device to ensure that an adequate seal is formed. Repetitive integration and removal of the microarray will confirm microarray integrity. Finally, we want to incorporate cells and determine their responses to soluble factor gradients while ensuring cell viability in the channels. Initial calculations have shown that minimal fluid shear stress will be induced upon the cells, as shown in Appendix B.

REFERENCES

[1] NIH. (2005, *The Life and Death of a Neuron*. Available: http://www.ninds.nih.gov/disorders/brain_basics/ninds_neuron.htm

[2] NINDS. (2004, *Parkinson's Disease Backgrounder*. Available: http://www.ninds.nih.gov/disorders/parkinsons_disease/parkinsons_disease_backgrounder.htm

[3] NIH. (2006, *Parkinson's Disease: Hope Through Research*. Available: http://www.ninds.nih.gov/disorders/parkinsons_disease/detail_parkinsons_disease.htm

[4] D. Y. Hwang*, et al.*, "Human ES and iPS cells as cell sources for the treatment of Parkinson's disease: current state and problems," *Journal of Cellular Biochemistry,* vol. 109, pp. 292-301, 2010.

[5] N. L. Jeon*, et al.*, "Generation of solution and surface gradients using microfluidic systems," *Langmuir,* vol. 16, pp. 8311-8316, 2000.

[6] N. L. Jeon*, et al.*, "Microfluidic gradient devices," ed: Google Patents, 2011.

[7] S. K. W. Dertinger*, et al.*, "Generation of gradients having complex shapes using microfluidic networks," *Analytical Chemistry,* vol. 73, pp. 1240-1246, 2001.

[8] V. V. Abhyankar*, et al.*, "Characterization of a membrane-based gradient generator for use in cell-signaling studies," *Lab Chip,* vol. 6, pp. 389-393, 2006.

[9] T. M. Keenan*, et al.*, "Microfluidic "jets" for generating steady-state gradients of soluble molecules on open surfaces," *Applied physics letters,* vol. 89, p. 114103, 2006.

[10] D. J. Beebe and V. V. Abhyankar, "Microfluidic platform and method of generating a gradient therein," ed: Google Patents, 2008.

[11] S. K. Sia and G. M. Whitesides, "Microfluidic devices fabricated in poly (dimethylsiloxane) for biological studies," *Electrophoresis,* vol. 24, pp. 3563-3576, 2003.

[12] G. M. Whitesides, "The origins and the future of microfluidics," *Nature,* vol. 442, pp. 368-373, 2006.

[13] S. Kim*, et al.*, "Biological applications of microfluidic gradient devices," *Integr. Biol.,* 2010.

[14] R. S. Ashton*, et al.*, "High Throughput Screening of Gene Function in Stem Cells Using Clonal Microarrays," *Stem Cells,* vol. 25, pp. 2928-2935, 2007.

[15] Sigma-Aldrich. (1997, *Albumin, Bovine*. Available: http://www.sigmaaldrich.com/etc/medialib/docs/Sigma/Product_Information_Sheet/a4919pis.Par.0001.File.tmp/a4919pis.pdf

[16] C. Geankoplis, *Transport Processes and Unit Operations*, Third ed., 1993.

[17] S. Bird, *Transport Phenomena Revised Second Edition*: John Wiley & Sons, 2007.

[18] D. J. Beebe*, et al.*, "Physics and applications of microfluidics in biology," *Annual review of biomedical engineering,* vol. 4, pp. 261-286, 2002.

[19] L. Kim*, et al.*, "Microfluidic arrays for logarithmically perfused embryonic stem cell culture," *Lab Chip,* vol. 6, pp. 394-406, 2006.

[20] B. G. Chung and J. Choo, "Microfluidic gradient platforms for controlling cellular behavior," *Electrophoresis,* 2010.

APPENDIX

Appendix A: Product Design Specifications

Microfluidic Platform for Culture and Live Cell Imaging of Cellular Microarrays
(Microfludic_Platform)

Project Design Specifications
December 14th, 2011

Group Members: Sarah Reichert, Anthony Sprangers, Alex Johnson, and John Byce

Advisor: Dr. John Puccinelli
Client: Dr. Randolph Ashton

Function:

Cellular microarrays contain populations of living cells that are spatially separated from one another. Because of the numerous discrete populations, these devices are beneficial in high-throughput screening applications. We aspire to expand the utility of cellular microarrays by designing a way to integrate them with microfluidic platforms that are compatible with a standard microscope stage. Along with fitting in the stage, the platforms must be able to generate concentration gradients across the field of flow, form a watertight seal, and be reusable in order for the devices to be effective. By accomplishing this, our client will be able to perform live-cell imaging and high-throughput analysis to determine how various culture conditions effect stem cell differentiation.

Client Requirements:

- A prototype microfluidic platform that can:
  - Generate concentration gradients across a cellular microarray
  - Form a water-tight seal with a microscope slide containing the microarray
  - Be reusable for multiple cellular microarrays
  - Fit on top of a microscope stage and be used for live-cell imaging

1. Physical and Operational Characteristics

A. ***Performance Requirements:*** The device must be able to house cellular microarrays and enable a concentration gradient of fluids to continuously flow, without leakage, while the arrays are imaged with a confocal microscope.
B. ***Safety:*** The apparatus cannot be harmful to the cells that it will contain or the researchers who will be working with it.

C. ***Accuracy and Reliability:*** An accurate and reliable concentration gradient must be able to be established and maintained across the field of flow. This will ensure that the data obtained from experiments utilizing the microfluidic platform will be repeatable and that the results are truly representative of how certain conditions effect stem cell differentiation.
D. ***Life in Service:*** The platform must be able to be continuously used for the duration of various types of stem cell experiments, which typically range from 1 to 10 days in length. The molds to create the platforms should be capable of being reused for 10 PDMS devices.
E. ***Shelf Life:*** When not in use, the device mold will be stored on a laboratory shelf at 20 °C and standard pressure. It must be capable of retaining its full functionality at these conditions for up to two years.
F. ***Operating Environment:*** While experiments are running, the temperature of the apparatus will be 20-37 °C. During imaging, the laser used may increase the temperature to slightly above 37 °C; however, this change is not expected to be significant and therefore should not affect the efficacy of the device. As testing will be performed in a standard laboratory, humidity and pressure will be within the typical ranges for this type of environment. In order to sterilize the device, it will be autoclaved, temporarily exposing it to high pressure saturated steam at 121 °C, or washed with sterilizing chemicals, which may potentially be corrosive.
G. ***Ergonomics:*** The platform should be easy to use by trained researchers and should not impose any physical strain on their part to assemble or disassemble for experiments.
H. ***Size:*** The maximum dimensions for the portion of the microfluidic device that will fit within the microscope stage for imaging are 158 x 105 mm. The device should be under 2.5 cm in height to fit within the stage area.
I. ***Weight:*** The device must weigh less than 0.5 kg, the maximum recommended load for the piezoelectric microscope stage that it will be mounted on for imaging.
J. ***Materials:*** The materials used must be biocompatible, nontoxic, and able to withstand sterilization techniques such as autoclaving and the use of sterilizing chemicals. Materials that have a history of use in microfluidic devices and entail simple fabrication and design processes are ideal.
K. ***Aesthetics, Appearance, and Finish:*** The portion of the apparatus that will contain the cellular arrays must be transparent so that the cells can be properly imaged and analyzed by researchers.

2. Production Characteristics

A. ***Quantity:*** One mold that can be used to create PDMS devices for use in multiple experiments is required.
B. ***Target Product Cost:*** If the device does not require temperature control for effective usage, then the target total manufacturing costs should be

less than $5,000. If temperature control is required, the costs will likely need to be between $10,000 and $20,000.

3. Miscellaneous

A. ***Standards and Specifications:*** There are no federal regulations that need to be met for this device; however, as the apparatus will be used with cultured cells, it must adhere to standard cell culture protocols.
B. ***Customer:*** Intended customers for this device will desire a microfluidic platform that can be easily applied, removed, and reused on cellular microarrays. Other devices in the competitive market are not removable and thus limit the potential for expansion of cell lines after experimentation.
C. ***Patient-related Concerns:*** Induced pluripotent and embryonic stem cells will be seeded in this apparatus. As a result, it must be able to be sterilized between uses. There are no concerns regarding data storage or confidentiality involved with this project, as the subjects are not patients.
D. ***Competition:*** Several research efforts have used PDMS microfluidic devices to deliver soluble factors to cells and establish concentration gradients (pioneered by Whitesides *et al*., 2000). One notable competing device developed for a similar research goal was patented by David J. Beebe *et al.* in 2007. This apparatus is titled *Microfluidic platform and method of generating a gradient therein*, and implements a single microfluidic channel with porous membranes and source/sink action to generate a gradient of particles. A comparable device using a source and sink gradient bridge titled *Microfluidic gradient devices* was developed and patented by Noo Li Jeon *et al.* in 2011.

Appendix B: Transport Equations

Diffusion within serpentine channels

Diffusion through the serpentine channels was modeled using COMSOL which was then verified using transport phenomena equations. We chose to use bovine serum albumin (BSA) as a model protein due to its large size (66.4 kDa) [15]. We will be using proteins that are smaller than BSA, so BSA is modeling a very maximal situation. The diffusion coefficient of BSA is reported to be $D = 6.81 \times 10^{-11}$ m^2/s [16]. Diffusion follows Fick's law, relating the velocity vector of the fluid to the diffusion coefficient and concentration gradient, which can be seen as equation 1 [17].

Equation 1- ——

This is greatly simplified if diffusion is present in only one direction. Luckily, in our case diffusion is only important in the direction perpendicular, but in the same plane as the flow. Using this simplification, it is easy to solve for the time it takes particles to diffuse from the boundary layer of two neighboring streams, to the opposite channel wall. This equation can be seen as equation 2 [16, 18].

Equation 2- —

Here, d is the distance to diffuse and D is the diffusion coefficient. Applying this to our microfluidic device where d = 25 microns (50 microns divided by two since there are two neighboring streams in one channel) and $D = 6.81 \times 10^{-11}$ m^2/s (BSA diffusivity) yields a time of 9.18 seconds for the establishment of diffusion equilibrium.

Since we know the flow rate of our fluid, we can determine how far this mixing stream will travel down the serpentine channel using the diffusion time reported above. We can then compare this distance to the known distance of a single serpentine channel, which is 10.55mm. If the distance traveled by the mixing fluid is less than the distance of a serpentine channel, then we know the flow rate will allow for adequate diffusion of molecules in the serpentine channel before the next branching point. However, if the distance traveled by the mixing fluid is greater than the length of a serpentine channel, then we need to lower the flow rate to allow for more time in the serpentine channel for adequate diffusion.

Since our device utilizes two inputs at an equal flow rate, the greatest flow rate will be in the first branch of serpentine channels (since the two input flow rates divide into three serpentine channels, each serpentine channel will have a flow rate equal to 2/3 the input flow rate). Further branching within the Christmas tree gradient generator will result in a decreased flow rate for each successive level, which will allow for more time for diffusion. Thus, it is appropriate to model the diffusion solely within the first three serpentine channels since these will experience the least time to achieve diffusion equilibrium.

A flow rate of 0.165 L/minute resulted in a distance traveled of 10.09 mm by the mixing fluid. This is the maximum flow rate which still allows for proper diffusion within the length of a single serpentine channel (since 10.09 mm is less than 10.55 mm). This translates to an inlet flow rate of 0.248 L/minute.

Fluid shear stress on cells

In pressure-driven flow systems, such as our microfluidic device, the pressure drop, ΔP, is related to the volumetric flow rate, Q, and fluid resistance, R, via equation 3 [17, 19].

Equation 3-

In our specific system the cell culture channels have a rectangular cross-section. Fluid resistance for this type of cross-section is described by equation 4 [18,19].

Equation 4-

Here, h = channel height, w = channel width, L = channel length and = fluid viscosity. For simplicity, this can be modeled using equation 5.

Equation 5-

We assumed our flow profile through the cell culture channels would be well-approximated by laminar flow through a narrow slit. The velocity profile through this type of slit is described equation 6 [17].

Equation 6-

Using Newton's law of viscosity [17], equation 7, we can solve for the momentum flux, .

Equation 7-

Substituting equation 5 into equation 6 and taking the derivative of the velocity profile allows us to solve for the max shear stress which occurs at the channel wall, i.e. when x = w. This results in equation 8.

Equation 8-

Using this final equation, the viscosity of water, h = 250 microns, and the flow rate discussed in the above diffusion section, cells in this type of system would experience a shear stress of 0.006 dynes/cm^2. This is well below typical physiological shear stresses experience by cells during normal blood flow which is approximately 2 dynes/cm^2 [20]. Thus, adverse affects due to shear stress will not be a problem in this design.